Enterocolitis induced by autoimmune targeting of enteric glial cells: A possible mechanism in Crohn's disease?

Anne Cornet*†, Tor C. Savidge†‡, Julie Cabarrocas*, Wen-Lin Deng‡, Jean-Frederic Colombel§, Hans Lassmann¶, Pierre Desreumaux§, and Roland S. Liblau*‖

*Institut National de la Santé et de la Recherche Médicale U546 and Immunology Laboratory, Pitié-Salpêtrière Hospital, Paris 75013, France; ‡Combined Program in Pediatric Gastroenterology and Nutrition, Massachusetts General Hospital and Harvard Medical School, Charlestown, MA 02129; §Inflammatory Bowel Disease Laboratory, Equipe Mixte Institut National de la Santé et de la Recherche Médicale-Université, Centre Hospitalo-Universitaire Lille 59000, France; and ¶Department of Neuroimmunology, Brain Research Institute, University of Vienna, 1090 Vienna, Austria

Communicated by Frederick M. Ausubel, Harvard Medical School, Boston, MA, September 6, 2001 (received for review March 8, 2001)

Early pathological manifestations of Crohn's disease (CD) include vascular disruption, T cell infiltration of nerve plexi, neuronal degeneration, and induction of T helper 1 cytokine responses. This study demonstrates that disruption of the enteric glial cell network in CD patients represents another early pathological feature that may be modeled after CD8$^+$ T cell-mediated autoimmune targeting of enteric glia in double transgenic mice. Mice expressing a viral neoself antigen in astrocytes and enteric glia were crossed with specific T cell receptor transgenic mice, resulting in apoptotic depletion of enteric glia to levels comparable in CD patients. Intestinal and mesenteric T cell infiltration, vasculitis, T helper 1 cytokine production, and fulminant bowel inflammation were characteristic hallmarks of disease progression. Immune-mediated damage to enteric glia therefore may participate in the initiation and/or the progression of human inflammatory bowel disease.

Astrocytes represent the most abundant glial cells of the central nervous system (CNS). Their primary role is to provide metabolic, trophic, and protective support for neurons, in addition to axonal guidance during development (1, 2). They also play a major role in maintaining the blood–brain barrier (2–4) and have the potential to participate in inflammatory and antigen-specific immune responses. Indeed, they produce chemokines (5), as well as proinflammatory and regulatory cytokines (1, 2, 6, 7). Moreover, astrocytes express MHC class I molecules and can be induced to express class II molecules, as well as CD80 and CD86 costimulatory molecules both *in vitro* and *in vivo* (8, 9). As a result, they can process and present self or foreign antigens to naive or effector CD4$^+$ or CD8$^+$ T cells *in vitro* (9–12) and therefore may contribute to the initiation and/or spread of autoimmune responses *in vivo* (13).

Enteric glial cells share anatomical, structural, and electrophysiological properties with astrocytes (14–17). They therefore appear to represent the glial cell counterpart of astrocytes in the enteric nervous system. It also has been suggested that enteric glia participate in intestinal immune responses, but direct evidence is lacking (18, 19). Information is still scarce regarding the physiological functions of these cells and their potential role in disease development.

A recent report has shown that genetic ablation of enteric glia results in a lethal gut pathology associated with disruption of mucosal integrity, hemorrhagic necrosis, and inflammation (20, 21). To examine whether disruption of the enteric glial cell network may result as a consequence of autoimmune-mediated targeting of this cell type in the gastrointestinal tract, we generated a double transgenic mouse model in which a viral (neoself) antigen is specifically expressed in astrocytes and enteric glia, and in which most CD8$^+$ T cells are specific for the neoself antigen. These mice rapidly display a disruption of the mucosal integrity and submucosal vascular lesions, which subsequently develops into a fulminant enterocolitis. Because these lesions are reminiscent of some pathological features of Crohn's disease (CD), a human inflammatory bowel disease (IBD) of unknown etiology, we hypothesized that a disruption of enteric glial cell populations could contribute to the pathophysiology of CD. The present study shows that enteric glial cell populations are similarly disrupted in CD, before the onset of intestinal inflammation, suggesting that this defect may contribute to the onset and/or perpetuation of intestinal inflammation.

Materials and Methods

Glial Fibrillary Acidic Protein (GFAP)-Hemagglutinin (HA) Gene Construct. We used the GFAP promoter and enhancer to direct the expression of the influenza virus A/PR8/34 HA to CNS astrocytes and enteric glial cells (20–23) (Fig. 1*a*). The *LacZ* gene was excised from pGfa2-Lac1 plasmid (22) by *Bam*HI digestion and replaced by a 1.7-kb *Bam*HI fragment containing HA sequences. The GFAP-HA gene construct (4.4 kb) was isolated from vector sequences through *Bgl*II digestion and microinjected into the male pronucleus of fertilized (DBA2 $\times$ C57Bl/6)F_2 eggs at Service d'Expérimentation Animale et de Transgénèse (Villejuif, France).

Mice. Tail DNA from the GFAP-HA offspring was screened either by Southern blot analysis of *Bam*HI-digested samples using a 1.7-kb HA probe or by PCR amplification (HA1 forward primer: 5′-GTGAGATCATGGTCCTACATT-3′; HA2 reverse primer: 5′-TCCTGACGTATTTTGGGCACT-3′). Three of six founders transmitted the transgene and showed mRNA expression of HA in the CNS. All experimental animals used in this study originated from line 21, backcrossed at least five times onto the BALB/c background. CL4-TCR transgenic mice express a HA512–520-specific, K^d-restricted T cell antigen receptor (TCR) on 90–96% of their mature CD8$^+$ T cells (24, 25). Identification of the CL4-TCR transgenic mice was made by PCR (forward primer: 5′-GCAGGGCTGAAAGAACAGCAA-3′; reverse primer: 5′ GCT-TCCTCCAGAATTTGAGGC-3′). The CL4-TCR transgenic line was backcrossed at least six times onto the BALB/c background. BALB/cByJ (H-2$^{d/d}$) and C57BL/6 (H-2$^{b/b}$) mice were purchased from IFFA-CREDO (Larbresle, France). For depletion of CD8$^+$ T cells (GFAP-HA $\times$ CL4)F_1 double transgenic mice were injected i.p. with 50 μg of a rat anti-mouse CD8 mAb (YTS 169, kindly provided by H. Waldmann, University of Oxford, Oxford, U.K.) or purified rat IgG (Sigma) at postnatal days 2, 4, and 6. All animal experiments were performed in accordance with the National

Abbreviations: CD, Crohn's disease; CNS, central nervous system; GFAP, glial fibrillary acidic protein; HA, hemagglutinin; IBD, inflammatory bowel disease; RT-PCR, reverse transcriptase–PCR; TCR, T cell antigen receptor; UC, ulcerative colitis.

†A.C. and T.C.S. contributed equally to this work.

‖To whom reprint requests should be addressed at: Institut National de la Santé et de la Recherche Médicale, U546 Faculté de Médecine Pitié-Salpêtrière, 105 Boulevard de l'Hôpital, Paris 75013, France. E-mail: 106063.1005@compuserve.com.

The publication costs of this article were defrayed in part by page charge payment. This article must therefore be hereby marked "*advertisement*" in accordance with 18 U.S.C. §1734 solely to indicate this fact.

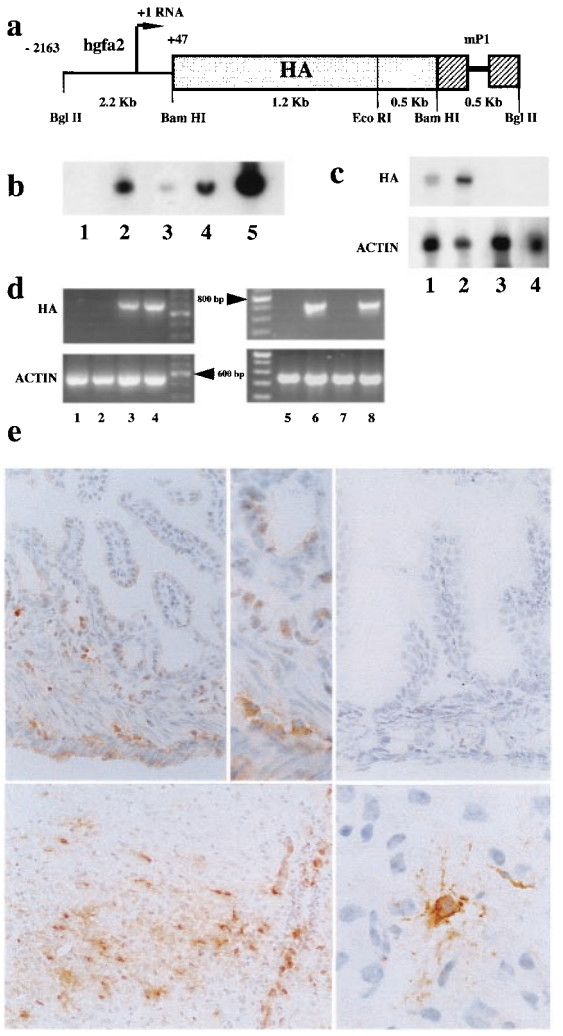

Fig. 1. GFAP-HA transgenic mice: transgene construct and expression. (*a*) DNA fragment containing the 1.7-kb HA coding sequence placed downstream from the *Gfap* promoter and upstream of a 0.5-kb segment of the mouse protamine-1 gene (*mP1*), which provides RNA splicing (thin line) and polyadenylation signals. (*b*) Southern blot analysis of *Bam*HI-digested genomic DNA from nontransgenic (lane 1) and transgenic (lane 2) progeny of founder GFAP-HA 21. Lanes 3–5: DNA from a nontransgenic mouse supplemented with 1, 10, and 100 copies of transgene per genome, respectively. (*c*) Northern blot analysis of 60 μg total RNA from brain (lane 1), spinal cord (lane 2), thymus (lane 3) from a transgenic mouse and brain from a nontransgenic littermate (lane 4) using either HA (*Upper*) or β-actin (*Lower*) probes. (*d*) HA (*Upper*) and β-actin (*Lower*) mRNA expression assessed by PCR amplification of cDNA from thymus (lane 1), heart (lane 2), brain (lane 3), spinal cord (lane 4), and small intestine from transgenic (lanes 6 and 8) and nontransgenic (lanes 5 and 7) mice. Fragments of 710 and 540 bp were expected for HA and β-actin, respectively. (*e*) Immunocytochemical detection of HA protein expression on frozen sections: (*Upper Left*) GFAP-HA transgenic animal with HA expression in the submucosal and myenteric plexus ($\times$450); (*Upper Center*) higher magnification ($\times$1,000), HA was expressed mainly in enteric nerve plexi; (*Upper Right*) control mouse, no HA gut expression ($\times$450); (*Lower Left*) GFAP-HA transgenic animal, spinal cord, HA expression in astrocytes ($\times$450); (*Lower Right*) GFAP-HA transgenic animal, high magnification of an HA-expressing astrocyte in the brain ($\times$1,300).

Institutes of Health Guidelines and had local committe approval (Pitié-Salpêtrière University Hospital).

RNA Analyses. For Northern blot analysis, 60 μg of glyoxal-treated total RNA (RNAzol B; Bioprobe International, Richmond, CA) was separated by agarose gel electrophoresis and transferred onto nylon membrane (Amersham Pharmacia). Blots were hybridized with [γ-^{32}P]dCTP-labeled HA probe for 15 h at 42°C in 50% formamide, 0.5% SDS, 5 $\times$ SSC, and 5 $\times$ Denhart's solution, washed under high stringency (four times for 20 min at 62°C in 0.1 $\times$ SSC, 0.5% SDS) and analyzed by autoradiography. Uniform RNA loading was confirmed by using a mouse β-actin probe. Quantitative reverse transcriptase–PCR (RT-PCR) analysis of cytokine gene expression was performed as described (26). Oligo(dT)-primed cDNA was amplified with 50 pmol of primer for 30 cycles. Primer sets specific to HA1, HA2, mouse β-actin (CLONTECH), IL-2, IL-4, IL-10, and IFN-γ were used. PCR results were expressed as the median numbers of cytokine cDNA molecules per 10^2 molecules of β-actin.

Histology and Immunohistochemistry. Standard paraffin hematoxylin/eosin-stained sections were used for histopathology. Immunohistochemistry was performed with the biotin/avidin system using anti-CD3 (CD3–12, Serotec); anti-CD45 (30-F11, PharMingen); anti-GFAP monoclonal (G-A-5, Roche Molecular Biochemicals) or polyclonal (Z334, Dako), anti-S-100 (Dako), or PGP9.5 (Biogenesis, Bournemouth, U.K.) antibodies. Frozen sections were used for HA and CD8 immunohistochemistry by using R46αPR8 (kindly provided by N. Escriou, Pasteur Institute, Paris) and clone 53–6.7 (PharMingen) antibodies, respectively. Double immunohistochemistry was performed for CD3 and GFAP by using diaminobenzidine (brown) and 3-amino-9-ethylcarbazol (red) as substrates, respectively. For quantitative determination, the total number and apoptotic enteric glia were measured as described (27). GFAP$^+$ enteric glial cells were counted in three jejunal cross sections per animal. Counts were performed separately in myenteric and submucosal plexi.

Patients. The 95 patients enrolled in the study gave their informed consent and the study was approved by the local ethical committee. The diagnosis of CD and ulcerative colitis (UC) was established by using usual criteria (26). Healthy and involved ileal and colonic biopsies were taken from 43 patients with CD (26 female/17 male; mean age 35 years; range 18 to 54 years). Biopsies were taken either during endoscopy (n = 14) or surgery (n = 29). The mean duration of CD was 8.5 years. Surgery in patients with CD was performed because of disease-related complications, i.e., symptomatic stenosis (25 cases) and fistula (four cases). No patients with CD received immunosuppressive therapy, five with an active disease were treated with steroids and six by 5-ASA. Twenty-eight patients with CD were not treated at the time of study. Healthy and involved colonic biopsies also were taken from 23 patients with UC (14 female/nine male; mean age 36 years; range 21 to 64 years) during endoscopy (n = 14) or surgery (n = 9). The mean duration of UC was 10.4 years. The nine patients with UC underwent surgery because of disease resistance to steroids (n = 7) or cyclosporin (n = 2). The 14 other patients with UC had a quiescent disease and were not treated, except for five patients receiving 5-ASA. As controls, healthy ileal or colonic biopsies were taken from 29 patients suffering from irritable bowel syndrome (n = 13, eight female/five male; mean age 51 years; range 28 to 63 years), sigmoiditis (n = 4, four male; mean age 62 years; range 48 to 72 years), and cancer of the right colon (n = 12, 12 male; mean age 64 years; range 55 to 74 years). Tissue GFAP levels (ng/mg protein) were measured in a blinded fashion in patient and transgenic mouse gut tissues by Western blot analysis and ELISA as described (20, 21).

Results

Expression of Influenza Virus HA in the CNS and Enteric Nervous System of GFAP-HA Transgenic Mice. Founder GFAP-HA mice were tested for successful integration of the full-length HA transgene (Fig. 1*a*) by Southern blot analysis of tail DNA. Line 21 showed the highest expression of HA and was selected for further study. Southern blot analyses of genomic DNA showed that an estimated 20 copies of the transgene were integrated at a single chromosomal

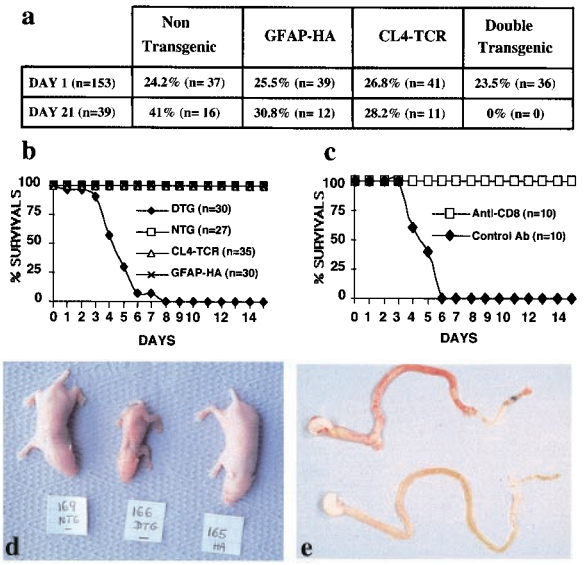

Fig. 2. (GFAP-HA × CL4-TCR)F_1 double transgenic (DTg) mice develop a fatal disease. (*a*) Observed distribution of the four different genotypes in pups from crosses of heterozygous CL4-TCR and GFAP-HA Tg mice at days 1 and 21. The frequency of DTg mice at day 21 was significantly less than the expected 25% ($P < 0.005$). (*b*) Survival of subgroups of (GFAP-HA × CL4-TCR)F_1 DTg, nontransgenic (NTg), and single CL4-TCR or GFAP-HA Tg littermates. (*c*) Survival of (GFAP-HA × CL4-TCR)F_1 DTg mice treated with a rat anti-CD8 antibody ($n = 10$) or control rat IgG ($n = 10$). (*d*) Phenotypical appearance of (GFAP-HA × CL4-TCR)F_1 DTg (166), NTg (169), and GFAP-HA Tg (165) littermates at day 5 of postnatal life. (*e*) Macroscopic appearance of the gastrointestinal tract of a (GFAP-HA × CL4-TCR)F_1 DTg mouse (*Upper*) and a NTg littermate (*Lower*) at day 5.

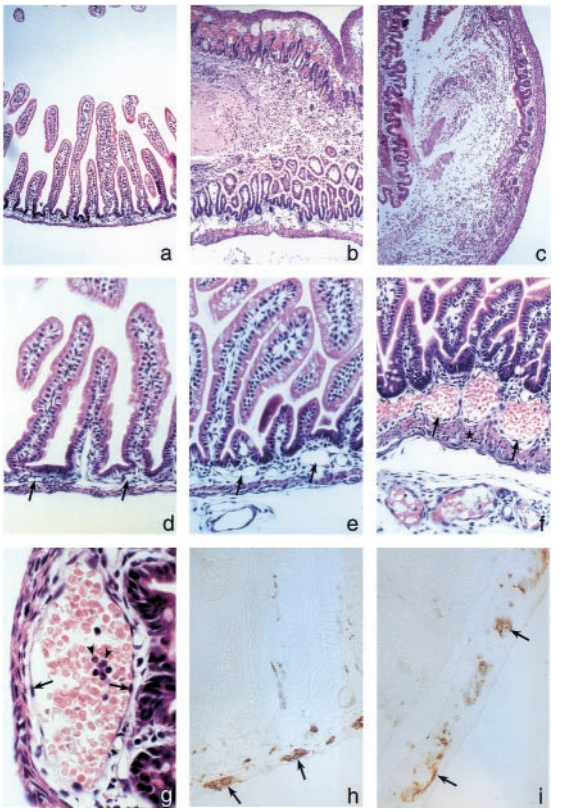

Fig. 3. Jejuno-ileo-colitis develops in (GFAP-HA × CL4-TCR)F_1 double transgenic mice. (*a*) Hematoxylin/eosin-stained section showing normal jejunal histology in a 7-day-old GFAP-HA transgenic mouse. Late-stage lesion of the jejunum (*b*) and colon (*c*) in double transgenic mice with mucosal and submucosal edema, epithelial damage, mucosal inflammation, hemorrhage, and necrosis that severely perturbed the crypt-villous architecture and mucosal integrity (×40 for *a–c*). (*d*) Normal jejunal histology in GFAP-HA trangenic mice. (*e* and *f*) Pathology in double transgenic mice was initially observed in submucosal capillaries and blood vessels (arrows) (×100 for *d–f*); asterisk in *f* indicates smooth muscle thickening; (*g*) with vasodilation, erythrostasis, endothelial hypertrophy and hyperplasia (arrows), and neutrophil (arrowheads) and lymphocyte infiltration. (*h*) PGP9.5 immunostaining in the jejunal myenteric plexus in GFAP-HA transgenic and (*i*) double transgenic mice (×400 for *g–i*).

site and were stably transmitted (Fig. 1*b*). Northern blot analysis of transgene expression in multiple tissues (brain, spinal cord, thymus, liver, small bowel, heart) from adult mice showed restricted expression in brain and spinal cord only (Fig. 1*c*). However, using RT-PCR, HA expression was detected in small and large intestine of transgenic mice. No detectable expression was recorded in other peripheral tissues, including relevant sites for tolerance induction e.g., thymus (Fig. 1*d*) and spleen. Evidence that HA protein was expressed in transgenic animals was provided by immunohistochemistry, restricted to a subpopulation of CNS astrocytes (Fig. 1*e*) and glia within the enteric nervous system (Fig. 1*e*). No expression was found in other components of the peripheral nervous system.

Single GFAP-HA transgenic mice survived for more than 1 year, bred normally, and showed no clinical or pathological abnormalities as a consequence of expression of the viral neoself antigen. No signs of inflammation were observed at sites of HA expression such as the brain, spinal cord, or gut from pups or adult (up to 12 months of age) mice (see Fig. 3 and data not shown). Thus, GFAP-HA transgenic mice appeared to be functionally tolerant to glial cell-expressed HA, showing no evidence of spontaneous autoimmunity.

(GFAP-HA × CL4-TCR)F_1 Double Transgenic Mice Die Prematurely. To analyze T cell tolerance to an immunodominant MHC class I-restricted epitope of HA in H-2^d mice (28), GFAP-HA transgenic mice were bred with CL4-TCR transgenic mice, in which most $CD8^+$ T cells are specific for the K^d:$HA_{512–520}$ complex. Crossing of these mice generate double transgenic animals in which the vast majority of $CD8^+$ T cells target a glial cell-specific neoself antigen. Surprisingly, although 25% of offspring were expected to be double transgenic, none were detected among 39 pups at 3 weeks of age (Fig. 2*a*; $P < 0.005$ χ^2 test). At birth, however, the genotypes followed the expected Mendelian distribution (Fig. 2*a*; $P = 0.94$). Daily examination of 30 double transgenic mice revealed that all mice died by day 8 of life, with a mean survival time of 4.5 days (Fig. 2*b*).

Both male and female double transgenic mice appeared normal at birth, but rapidly exhibited growth retardation and dehydration (Fig. 2*d*). No obvious paralysis or seizures were observed. Survival of 10 double transgenic mice derived under specific pathogen-free conditions (mean survival 4.4 days) was identical to conventionally raised mice, thereby excluding pathogenic bacteria and viruses as possible causes of death.

(GFAP-HA × CL4-TCR)F_1 Double Transgenic Mice Develop Intestinal Vasculitis and Fulminant Jejuno-Ileo-Colitis. Extensive macroscopic analyses of vital organs (CNS, heart, lung, liver, spleen, pancreas, kidney, adrenal, and gastrointestinal tract) of double transgenic mice revealed gross pathology in gut tissues only. The jejunum, ileum, and colon were distended and macroscopically inflamed and hemorrhagic (Fig. 2*e*). The gut lumen contained nonemulsified milk, which probably accounted for the failure of the mice to thrive. Inflammation and hemorrhage were patchy in the small and proximal large bowel, although ileal tissues were most severely affected with smooth muscle wall thickening, occasional ulcers, and transmural perforation (Fig. 3 *b*, *c*, and *f*).

Initial pathology involved the submucosal capillaries and blood

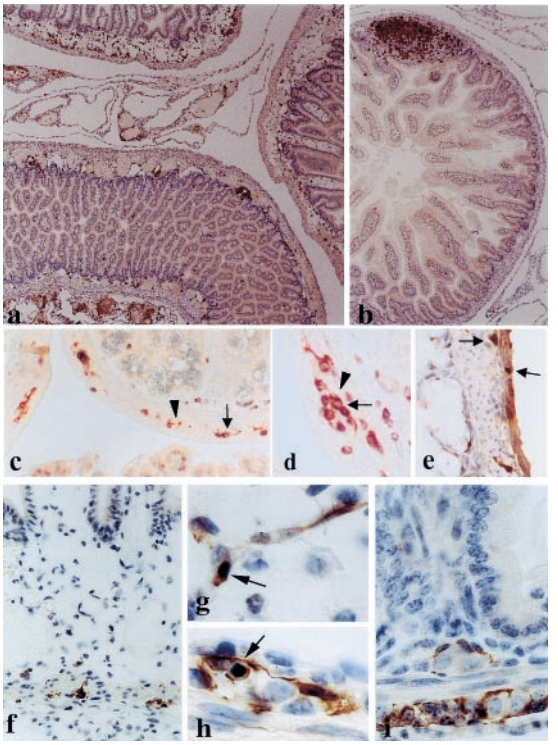

Fig. 4. Small intestine pathology in (GFAP-HA × CL4-TCR)F_1 double transgenic mice. (*a*) Five-day-old double transgenic pup with moderate inflammation in the gut wall, associated with edema and vasodilatation. Inflammation (anti-CD3) was also observed in the surrounding mesentery. (*b*) Nontransgenic littermate; normal gut architecture; T cells are concentrated mainly in lymph follicles (×90 for *a* and *b*). (*c* and *d*) Double transgenic animal, infiltration of the myenteric plexus with T cells (*c*, ×360; *d*, ×720); double staining with anti-CD3 (brown, arrows) and GFAP (red, arrowheads). (*e*) Double transgenic animal; immunohistochemistry with anti-CD8; infiltration of the muscular wall and the myenteric plexus by $CD8^+$ T cells (×360). (*f*) Double transgenic animal; $GFAP^+$ immunohistochemistry; edema and inflammation in the mucosa and submucosa; only a few $GFAP^+$ cells remain in the myenteric plexus (×450). (*g*) Double transgenic animal; apoptotic $GFAP^+$ cell in the submucosal plexus (×1,300). (*h*) Double transgenic animal; apoptotic $GFAP^+$ cell in the myenteric plexus (×1,300). (*i*) $GFAP^+$ enteric glial cells in the myenteric and submucosal plexi in a normal, nontransgenic animal (×1,000).

vessels, which showed vasodilation and erythrostasis (Fig. 3*i*). Progression of these changes included endothelial cell hypertrophy and hyperplasia, transmigration of leukocytes, formation of intravascular microthrombi, and local edema that resulted in a loss of submucosal architecture (Fig. 3 *b*, *c*, and *f*). Hemorrhage and edema initiated in the submucosa and later spread, severely disrupting the muscularis mucosae and externae and the intestinal mucosa (Fig. 3 *b*, *c*, and *e*).

Increased numbers of T lymphocytes, especially $CD8^+$ cells, were dispersed throughout the submucosa, and even infiltrated the muscularis externae (Fig. 4 *a* and *e*), where they juxtaposed $GFAP^+$ enteric glia (Fig. 4 *c* and *d*). The inflammatory process also spread to the mesentery where pronounced perivascular and diffuse inflammatory infiltrates were noted (Fig. 4*a*). By contrast, in littermate controls T cells were restricted to the mucosa, mainly within Peyer's patches (Fig. 4*b*).

Table 1. Apoptotic loss of $GFAP^+$ enteric glial cells in (GFAP-HA × CL4-TCR)F_1 double transgenic mice

Location	Cell type	NTg mice (n = 4)	GFAP-HA mice (n = 6)	DTg mice (n = 7)
Myenteric plexus	$GFAP^+$	94 ± 11.3	95 ± 10.2	62 ± 9.3*
	Apoptotic $GFAP^+$	0	0	2.5 ± 1.5†
Sumucosal plexus	$GFAP^+$	14.3 ± 3.3	16.3 ± 6.0	4.4 ± 2.1*
	Apoptotic $GFAP^+$	0	0	0.64 ± 0.69†

Number (mean ± SEM) of $GFAP^+$ cells per animal over a complete circumference of the jejunum. NTg, nontransgenic; DTg, double transgenic.
*The number of $GFAP^+$ cells is significantly reduced in the myenteric plexus (P = 0.0006, two-tailed Student's t test) and submucosal plexus (P = 0.004) of DTg mice as compared with control mice.
†Apoptotic $GFAP^+$ cells were only found in the intestine of DTg mice.

GFAP expression was prominent in enteric glia of the submucosal and myenteric plexi in control animals and was significantly reduced in double transgenic mice (Fig. 4 *f* and *i*; Table 1). Remaining $GFAP^+$ cells often displayed morphological alterations typical of apoptosis (Fig. 4 *g* and *h*; Table 1). Ablation of $GFAP^+$ enteric glial cells initiated and was most pronounced in the submucosal plexus (72% loss of $GFAP^+$ cells; Table 1). Enteric neuron numbers appeared unaffected by histology or immunostaining with PGP9.5 (Fig. 3 *h* and *i*). Apart from gut pathology, the only other microscopic abnormalities were focal destructive inflammatory lesions in the brains of 30% of 2- to 6-day-old animals (data not shown).

Jejuno-Ileo-Colitis in (GFAP-HA × CL4-TCR)F_1 Double Transgenic Mice Is a $CD8^+$ T Cell-Mediated Autoimmune Disease. To assess the role of T cells in initiating jejuno-ileo-colitis in double transgenic animals, several experiments were performed. First, histological analysis of H-$2^{d/d}$ double transgenic mice (n = 6) on postnatal day 1, i.e., before large numbers of T cells exit from the thymus and colonize secondary lymphoid organs, demonstrated no pathology at sites of HA expression. Second, GFAP-HA and CL4-TCR mice were separately crossed with C57BL/6 mice, then intercrossed to generate homozygous H-$2^{b/b}$ (GFAP-HA × CL4-TCR)F_1 double transgenic mice in which the HA peptide could not be presented to T cells because of the lack of K^d molecules. None of six such mice studied had clinical or histopathological signs of gut or CNS abnormality. Finally, in double transgenic H-$2^{d/d}$ mice (n = 10) injected with a depleting rat anti-CD8 mAb on days 2, 4, and 6 after birth, all mice survived for more than 2 weeks whereas control mice (n = 10) receiving nonspecific rat IgG died by day 6 (Fig. 2*c*). Collectively, these data show that the fatal autoimmune disease that develops in (GFAP-HA × CL4-TCR)F_1 double transgenic mice is mediated by HA-specific $CD8^+$ T cells.

To further investigate the phenotype of the pathogenic autore-

Table 2. Detection of cytokine production in the jejunum by quantitative RT-PCR analysis

Mice	IFN-γ	IL-2	IL-4	IL-10
Double transgenic (n = 4)	4.14 (0.8–6.0)*	0.09 (0–0.62)†	0.09 (0.05–0.11)‡	0.67 (0–8)†
Nontransgenic (n = 15)	0.58 (0.31–0.74)	0.06 (0.15–1.11)	1.32 (0.17–4.9)	1.13 (0–20)

Quantitative RT-PCR results are expressed as the median (95% confidence interval) of cytokine cDNA molecules per 10^2 molecules of β-actin.
*, P = 0.006 as compared with control nontransgenic mice.
†, Not statistically significant compared with control mice.
‡, P = 0.01 as compared with control mice.

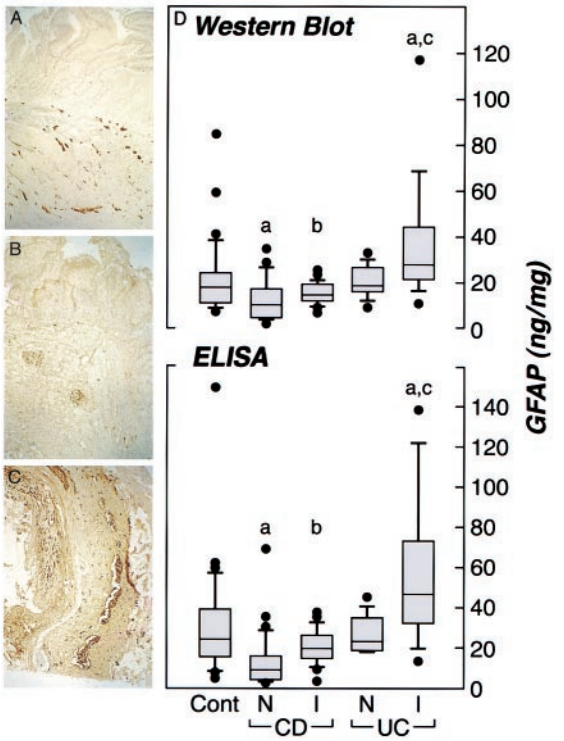

Fig. 5. GFAP$^+$ enteric glial cell populations in human IBD. (*A–C*) Immunohistochemistry for GFAP in control, involved CD and UC samples, respectively (×100). (*D*) Box plot demonstrating tissue GFAP levels (ng/mg protein) in clinical biopsies measured by Western blot and ELISA. Clinical groups have been nominated as histological normal controls (CONT; $n = 33$), noninvolved CD (CD-N; $n = 39$), involved CD (CD-I; $n = 23$), noninvolved UC (UC-N; $n = 10$), and involved UC (UC-I; $n = 15$). Ileal and colonic biopsies have been pooled because no significant differences were observed between the sites for the different groups. Significant differences (Mann–Whitney *U* test) from CONT are indicated as (*a*) included CONT vs. CD-N ($P = 0.0005$ and $P < 0.0001$ for Western blot and ELISA, respectively), and CONT vs. UC-I ($P = 0.0045$ and $P = 0.0064$ for Western blot and ELISA, respectively). *b* indicates a significant difference between CD-N and CD-I ($P = 0.0058$ and $P = 0.0001$ for Western blot and ELISA, respectively). *c* indicates a significant difference between UC-N and UC-I ($P = 0.023$ and $P = 0.0009$ for Western blot and ELISA, respectively). Significant differences also were recorded between CD-N and UC-N ($P = 0.024$ and $P = 0.0009$ for Western blot and ELISA, respectively) and CD-I and UC-I ($P = 0.009$ and $P = 0.0176$ for Western blot and ELISA, respectively).

active CD8$^+$ T cells, intestinal cytokine mRNA content was assessed by quantitative RT-PCR. Significantly higher levels of IFN-γ and lower levels of IL-4 mRNA were detected in double transgenic as compared with littermate control mice (Table 2). IL-10 and IL-2 mRNA levels were not significantly altered. The pathology is therefore associated with a type 1 cytokine profile.

Enteric Glial Cell Networks Are Severely Disrupted in Involved and Noninvolved Intestine of CD Patients. In view of the dramatic phenotype displayed after disruption of the enteric glial cell network in GFAP-HSV*tk* (20, 21) and (GFAP-HA × CL4-TCR)F_1 double transgenic mice described above, we examined whether similar abnormalities are also apparent in human IBD. Immunohistochemistry demonstrated an extensive GFAP$^+$ enteric glial cell network in human control biopsies. Although most readily detectable within the submucosal and myenteric plexi (Fig. 5*A*), enteric glial cell processes also extended into the mucosa. Immunolabeling of histologically normal, noninvolved ileal and colonic samples from CD ($n = 7$) patients were compared with control tissues from patients with no prior history of IBD ($n = 10$). Involved tissues from the same CD ($n = 9$) or UC ($n = 5$) patients also were examined to assess enteric glial cell reactivity after mucosal inflammation. Blind evaluation of GFAP$^+$ immunoreactive processes in these tissues indicated that both noninvolved and involved CD specimens demonstrated a diminished enteric glial cell network as compared with control or UC patients (Fig. 5 *A–C*), especially within the mucosa and submucosa. Quantitative immunohistochemical analyses using anti-S-100 antibodies, a second marker for enteric glia, correlated well with GFAP data, and also revealed significantly decreased staining in CD samples as compared with control tissues ($1.52 \pm 0.20\%$, $n = 8$ versus $3.05 \pm 0.68\%$, $n = 14$; $P = 0.037$, respectively). These findings were confirmed by ELISA and Western blot analysis specifically quantifying the 53-kDa form of GFAP, where significantly reduced levels of tissue GFAP were recorded in noninvolved biopsies from patients with CD ($n = 39$), as compared with UC ($n = 10$; $P = 0.0009$ and $P = 0.024$, for ELISA and Western blot respectively; Mann–Whitney *U* test) or controls ($n = 33$; $P < 0.0001$ and $P = 0.0005$, respectively) (Fig. 5*D*). Significantly less GFAP tissue levels were also recorded in CD as compared with UC samples in inflamed samples ($P = 0.009$ and $P = 0.0176$ for Western blot and ELISA, respectively). In addition, the glial cell reaction in response to tissue inflammation in clinical specimens (manifested as glial cell hypertrophy and up-regulation of GFAP expression) (1) was less pronounced in inflamed specimens from patients with CD ($n = 23$; 1.3-fold and 1.6-fold increase by Western blot and ELISA, respectively) compared with UC ($n = 15$; 1.6-fold and 2.1-fold increase, respectively) (Fig. 5*D*). Therefore, noninvolved ileal and colonic mucosa in CD patients is associated with a significantly diminished enteric glial cell network that responds poorly during inflammation when compared with UC. This disruption (45% reduction by Western blot analysis and 57% reduction by ELISA) is comparable to levels of ablation that result in a fulminant gastrointestinal inflammation in GFAP-HSVtk mice (20, 21) and (GFAP-HA × CL4-TCR)F_1 double transgenic mice, ranging from a 45–62% reduction as measured by Western blot and ELISA.

Discussion

Our results define a mechanism of intestinal inflammation involving a CD8$^+$ T cell-mediated cytotoxic autoimmune response directed against enteric glia, a subpopulation of the enteric nervous system. This immune reaction leads to extensive submucosal edema and vascular inflammation, eventually giving rise to a fulminant bowel inflammation and hemorrhagic necrosis.

Enteric glial cells express high levels of GFAP (a major component of the intermediate filaments of astroglial cells) and S-100 (14). These cells envelop enteric neuronal cell bodies and axon bundles (15), as well as intestinal blood vessels (18, 29), and extend into the intestinal mucosa (14, 20). In addition to shared phenotypic features with astrocytes, they probably perform other common functions (15–17). Normally, enteric glia constitutively express MHC class I molecules, whereas MHC class II expression is barely detectable (18, 30). We have previously shown that naive CL4-TCR CD8$^+$ T cells proliferate rapidly *in vitro* in response to HA peptide-pulsed astrocytes (12). Enteric glia may therefore directly activate naive CL4-TCR CD8$^+$ cells after homing into the intestinal submucosa. However, cross-presentation of HA by bone marrow-derived antigen-presenting cells in the mesenteric lymph nodes also could explain why the gut is predominantly affected in this double transgenic system (31). Once primed in the intestine, CD8$^+$ T cells probably acquire the ability to cross the blood-brain barrier and interact with HA-expressing astrocytes, although CNS lesions are infrequent in double transgenic mice because of their short survival time. Thus, only the enteric glial cell network is consistently affected by this autoimmune-mediated process.

It has been shown that CNS astrocytes induce endothelial cells to form tight junctions that confer blood-brain barrier properties (3). *In vivo* ablation of reactive CNS astrocytes results in pronounced interstitial edema and parenchymal infiltration with leukocytes (4). In addition, blood vessels are devoid of astrocyte endfeet and blood-brain barrier repair is severely impaired. A peripheral blood-

tissue barrier showing some similarities to the blood-brain barrier also exists in the intestine where the neuronal plexi are similarly impermeable to systemic macromolecules (32). At this site, $GFAP^+$ processes are associated with intestinal blood vessels both within the submucosa (18) and mesentery (29). Therefore, enteric glial cells likely control the integrity and permeability of the submucosal blood vessels. This hypothesis is supported by the observation that the initial vascular lesions in our double transgenic mouse model involves vasodilatation and leakage into the submucosa. Enteric glial cell processes also extend throughout the intestinal mucosa to the villus tips, where they probably contribute to mucosal secretions as well as regulate epithelial permeability. Indeed, selective *in vivo* depletion of enteric glial cells leads to disruption of mucosal integrity followed by severe mucosal inflammation (20, 21). In our model, epithelial damage could be secondary to glial cell ablation and/or to the local production of inflammatory cytokines such as IFN-γ (33).

Strict control of the intestinal immune response and antigenic load is required to provide a protective local immunity without inducing immunopathology. Indeed, increased intestinal epithelial permeability of luminal antigens (34) and/or inefficient regulation of the gut immune system (35) may lead to IBD. In most, but not all (36, 37), current models of IBD, an uncontrolled type 1 $CD4^+$ T cell response to uncharacterized intestinal microflora antigens is responsible for induction of the pathology (35, 38–40), although the possible contribution of autoreactive $CD8^+$ T cells recently has been underlined (41). In the present model, a well-defined autoantigen expressed on enteric glial cells is the target of cytotoxic $CD8^+$ T cells.

The early onset and the fulminant course of the disease are reminiscent of human necrotizing enterocolitis (NEC), an inflammatory disease occurring in premature infants. The pathology of NEC is characterized by ischemic necrosis with frequent hemorrhage, extensive infiltration with neutrophils, and bacterial overgrowth. Enteric nervous system lesions in NEC are characterized by a parallel loss of neurons and glial cells in myenteric and submucosal plexi (42, 43), initially occurring in the antimesenteric intestinal side where ischemic lesions are more likely to occur. As such, these events are different from those generated in our mouse model because this is caused by specific autoimmune targeting of enteric glia while, during the study period, enteric neurons remain relatively unaffected.

In humans, pathogenic autoimmune reactions directed toward the enteric nervous system may represent a primary cause of Chagas disease-associated and paraneoplastic intestinal pseudo-obstruction. However, in these conditions, the main cellular targets are enteric neurons. Although autoantibodies against enteric neurons have been detected, the involvement of autoreactive T cells is highly probable as shown for other paraneoplastic neurological diseases (44, 45). In CD, it has long been known that submucosal and transmural inflammation is associated with lesions of the enteric nervous system (19), although it is not known whether enteric glial cells play a role in the pathogenesis. In the present study, a disruption of enteric glial cells was found only in CD and not in UC. Ablation studies in transgenic mice now suggest that an abnormal enteric glial cell network in healthy intestinal tissues of patients with CD may contribute toward the onset of pathology and inflammation via disruption of intestinal barrier function and/or dysregulation of submucosal vascular function. The expression of MHC class I and class II molecules by enteric glial cells (18, 30), their close colocalization with infiltrating T cells (18), and the presence of classical granulomas in the submucosal and myenteric plexi in otherwise uninvolved areas (18, 46) suggest a possible role for this cell type in the propagation of CD. The ability of enteric glia to regulate submucosal vascular function is clearly relevant to CD as inflammatory microvasculature injury is an early and prominent feature of clinical specimens (47, 48). In light of these observations, the striking decrease in GFAP immunoreactive processes specifically in CD gut samples may even suggest that enteric glia are specifically targeted by immune or nonimmune (e.g., viral) mechanisms.

We thank M. Touchard and F. Ferron for technical assistance, and Drs. N. Bercovici, N. Cerf-Bensussan, and D. Guy-Grand for help and advice. This work was supported by grants from the Institut National de la Santé et de la Recherche Médicale, The French Research Ministry, and the French MS Society (Association pour la Recherche sur la Sclerose en Plaques) to R.S.L., and by the Leukemia Research Fund, Crohn's and Colitis Foundation, Center for the Study of Inflammatory Bowel Disease (PODK43351B10), and National Institutes of Health Grants RO1-HD31852, PO1-DK33506, P30-DK40561, and R37-HD12437 (to T.C.S.).

1. Eddleston, M. & Mucke, L. (1993) *Neuroscience* **54,** 15–36.
2. Ridet, J. L., Malhotra, S. K., Privat, A. & Gage, F. H. (1997) *Trends Neurosci.* **20,** 570–577.
3. Janzer, R. C. & Raff, M. C. (1987) *Nature (London)* **325,** 253–257.
4. Bush, T. G., Puvanachandra, N., Horner, C. H., Polito, A., Ostenfeld, T., Svendsen, C. N., Mucke, L., Johnson, M. H. & Sofroniew, M. V. (1999) *Neuron* **23,** 297–308.
5. Ransohoff, R. M. & Tani, M. (1998) *Trends Neurosci.* **21,** 154–159.
6. Shrikant, P. & Benveniste, E. N. (1996) *J. Immunol.* **157,** 1819–1822.
7. Meinl, E., Aloisi, F., Ertl, B., Weber, F., de Waal Malefyt, R., Wekerle, H. & Hohlfeld, R. (1994) *Brain* **117,** 1323–1332.
8. Fontana, A., Fierz, W. & Wekerle, H. (1984) *Nature (London)* **307,** 273–286.
9. Nikcevitch, K. M., Gordon, K. B., Tan, L., Hurst, S. D., Kroepfl, J. F., Gardinier, M., Barrett, T. A. & Miller, S. D. (1997) *J. Immunol.* **158,** 614–621.
10. Sedgwick, J. D., Mössner, R., Schwender, S. & ter Meulen, V. (1991) *J. Exp. Med.* **173,** 1235–1246.
11. Soos, J. M., Morrow, J., Ashley, T. A., Szente, B. E., Bikoff, E. K. & Zamvill, S. S. (1998) *J. Immunol.* **161,** 5959–5966.
12. Cornet, A., Bettelli, E., Oukka, M., Cambouris, C., Avellana-Adalid, V., Kosmatopoulos, K. & Liblau, R. S. (2000) *J. Neuroimmunol.* **106,** 69–77.
13. Kojima, K., Berger, T., Lassmann, H., Hinze-Selch, D., Zhang, Y., Gehrmann, J., Reske, K., Wekerle, H. & Linington, C. (1994) *J. Exp. Med.* **180,** 817–829.
14. Jessen, K. R. & Mirsky, R. (1980) *Nature (London)* **286,** 736–737.
15. Gershon, M. D. & Rothman, T. P. (1991) *Glia* **4,** 195–204.
16. Bernstein, C. N. & Vidrich, A. (1994) *Glia* **12,** 108–116.
17. Broussard, D. L., Bannerman, P. G. C., Tang, C. M., Hardy, M. & Pleasure, D. (1993) *J. Neurosci. Res.* **34,** 24–31.
18. Geboes, K., Rutgeerts, P., Ectors, N., Mebis, J., Penninckx, F., Vantrappen, G. & Desmet, V. J. (1992) *Gastroenterology* **103,** 439–447.
19. Geboes, K. & Collins, S. (1998) *Neurogastroenterol. Mol.* **10,** 189–202.
20. Bush, T. G., Savidge, T. C., Freeman, T. C., Cox, H. J., Campbell, E. A., Mucke, L., Johnson, M. H. & Sofroniew, M. V. (1998) *Cell* **93,** 189–201.
21. Savidge, T. C., Bush, T. G., Wen-Lin, D., Johnson, M. & Sofroniew, M. V. (1999) *Microecol. Ther.* **28,** 81–92.
22. Brenner, M., Kisseberth, W. C., Su, Y., Besnard, F. & Messing, A. (1994) *J. Neurosci.* **14,** 1030–1037.
23. Schönrich, G., Kalinke, U., Momburg, F., Malissen, B., Hämmerling, G. J. & Arnold, B. (1991) *Cell* **65,** 293–304.
24. Morgan, D. J., Liblau, R. S., Scott, B., Fleck, S., McDevitt, H. O., Lo, D. & Sherman, L. A. (1996) *J. Immunol.* **157,** 978–983.
25. Bercovici, N., Heurtier, A., Vizler, C., Pardigon, N., Cambouris, C., Desreumaux, P. & Liblau, R. S. (2000) *J. Immunol.* **165,** 202–210.
26. Desreumaux, P., Brandt, E., Gambiez, L., Emilie, D., Geboes, K., Klein, O., Ectors, N., Cortot, A., Capron, M. & Colombel, J. F. (1997) *Gastroenterology* **113,** 118–126.
27. Schmied, M., Breitschopf, H., Gold, R., Zischler, H., Rothe, G., Wekerle, H. & Lassmann, H. (1993) *Am. J. Pathol.* **14,** 446–452.
28. Chen, W., Anton, L. C., Bennink, J. R. & Yewdell, Y. W. (2000) *Immunity* **12,** 83–93.
29. Björklund, H., Dahl, D. & Seiger, A. (1984) *Neuroscience* **12,** 277–287.
30. Koretz, K., Momburg, F., Otto, H. F. & Moller, P. (1984) *Am. J. Pathol.* **129,** 493–502.
31. Miller, J. F., Kurts, C., Allison, J., Kosaka, H., Carbone, F. & Heath, W. R. (1998) *Immunol. Rev.* **165,** 267–277.
32. Gershon, M. D. & Bursztajn, S. (1978) *J. Comp. Neurol.* **180,** 467–488.
33. Guy-Grand, D., DiSanto, J. P., Henchoz, P., Malassis-Séris, M. & Vassali, P. (1998) *Eur. J. Immunol.* **28,** 730–744.
34. Hermiston, M. L. & Gordon, J. I. (1995) *Science* **270,** 1203–1207.
35. Powrie, F. (1995) *Immunity* **3,** 171–174.
36. Boirivant, M., Fuss, I. J., Chu, A. & Strober, W. (1998) *J. Exp. Med.* **188,** 1929–1939.
37. Mizoguchi, A., Mizoguchi, E. & Bhan, A. K. (1999) *Gastroenterology* **116,** 320–326.
38. Asseman, C., Mauze, S., Leach, M. W., Coffman, R. L. & Powrie, F. (1999) *J. Exp. Med.* **7,** 995–1003.
39. Takeda, K., Clausen, B. E., Kaisho, T., Tsujimura, T., Terada, N., Förster, I. & Akira, S. (1999) *Immunity* **10,** 39–49.
40. Blumberg, R. S., Saubermann, L. J. & Strober, W. (1999) *Curr. Opin. Immunol.* **11,** 648–656.
41. Steinhoff, U., Brinkmann, V., Klemm, U., Aichele, P., Seiler, P., Brandt, U., Bland, P. W., Prinz, I., Zügel, U. & Kaufmann, S. H. E. (1999) *Immunity* **11,** 349–358.
42. Wedel, T., Krammer, H. J., Kühnel, W. & Sigge, W. (1997) *Pediatr. Pathol. Lab. Med.* **18,** 57–70.
43. Sigge, W., Wedel, T., Kühnel, W. & Krammer H. J. (1998) *Eur. J. Pediatr. Surg.* **8,** 87–94.
44. Benyahia, B., Liblau, R., Merle-Beral, H., Tourani, J. M., Dalmau, J. & Delattre, J. Y. (1998) *Ann. Neurol.* **45,** 162–167.
45. Albert, M. L., Darnell, J. C., Bender, A., Francisco, L. M., Bhardwaj, N. & Darnell, R. B. (1998) *Nat. Med.* **4,** 1321–1324.
46. Wakefield, A. J., Sankey, E. A., Dhillon, A. P., Sawyerr, A. M., More, L., Sim, R., Pittilo, R. M., Rowles, P. M., Hudson, M., Lewis, A. A. & Pounder, R. E. (1991) *Gastroenterology* **100,** 1279–1287.
47. Wakefield, A. J., Sawyerr, A. M., Dhillon, A. P., Pittilo, R. M., Rowles, P. M., Lewis, A. A. & Pounder, R. E. (1989) *Lancet* **2,** 1057–1062.
48. Murch, S. H., Braegger, C. P., Sessa, W. C. & MacDonald, T. T. (1992) *Lancet* **339,** 381–385.